Acta Crystallographica Section F
Structural Biology and Crystallization Communications
ISSN 1744-3091

Crystallization and preliminary crystallographic studies of a cysteine protease inhibitor from the human nematode parasite *Ascaris lumbricoides*

Sanling Liu,[a,b] Jianmei Dong,[a,b] Guoqiang Mei,[a,b] Guiyun Liu,[a] Wei Xu,[a] Zhong Su[a,b] and Jinsong Liu[a,b]*

[a]National Key Laboratory of Respiratory Disease, Guangzhou Institutes of Biomedicine and Health, Chinese Academy of Sciences, 190 Kaiyuan Avenue, Guangzhou Science Park, Guangzhou 510530, People's Republic of China, and [b]University of Science and Technology of China, Hefei, People's Republic of China

Correspondence e-mail: liu_jinsong@gibh.ac.cn

Received 17 October 2010
Accepted 3 December 2010

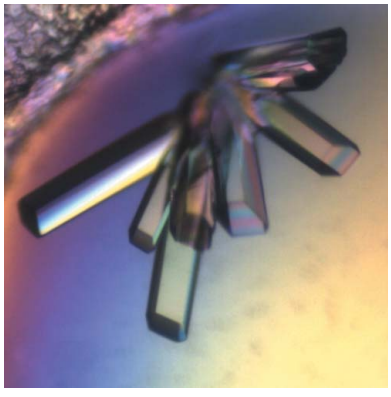

The cysteine protease inhibitor from *Ascaris lumbricoides*, a roundworm that lives in the human intestine, may be involved in the suppression of human immune responses. Here, the molecular cloning, protein expression and purification, preliminary crystallization and crystallographic characterization of the cysteine protease inhibitor from *A. lumbricoides* are reported. The rod-shaped crystal belonged to space group *C*2, with unit-cell parameters $a = 99.40$, $b = 37.52$, $c = 62.92$ Å, $\beta = 118.26^\circ$. The crystal diffracted to 2.1 Å resolution and contained two molecules in the asymmetric unit.

1. Introduction

The cysteine protease inhibitor (CPI) superfamily comprises a number of proteins that are present across species. CPIs mostly target family C1 (papain-like) cysteine proteases (Turk *et al.*, 1997). The cellular functions of CPIs include protection against unwanted proteolysis and regulation of intracellular and extracellular protein breakdown. For example, cathepsins (a mammalian version of family C1 cysteine proteases) have been shown to be involved in antigen presentation, apoptosis and bone remodelling in addition to their roles in lysosomal protein degradation (Chapman *et al.*, 1997; Honey & Rudensky, 2003; Turk *et al.*, 2002). Cathepsin function must be tightly regulated in order to avoid unnecessary activation. This regulation is provided through the binding of CPIs to cathepsins.

CPIs have been identified in many species of nematode parasites. They are believed to play important roles in the regulation of essential developmental events such as the moulting or the hatching of the worms (Lustigman *et al.*, 1992). Studies in recent years have demonstrated that protease inhibitors from parasitic worms are also able to modulate the functions of host immune systems (Gregory & Maizels, 2008). Further studies have shown that protease inhibitors of parasitic origin may influence the activity of cathepsin S, a cysteine protease that is important in antigen processing and presentation by dendritic cells, resulting in impaired immune responses (Dainichi *et al.*, 2001; Schonemeyer *et al.*, 2001). Owing to their immune-modulating properties, parasite protease inhibitors may have pharmaceutical value for the treatment of autoimmune and allergic diseases in humans.

We observed that a CPI from *Ascaris lumbricoides*, a roundworm that lives in the human intestine, strongly suppresses the activation of human immune cells (unpublished data). In this report, we performed a preliminary X-ray analysis of CPI from *A. lumbricoides* (Al-CPI) with the aim of understanding its three-dimensional structure.

2. Materials and methods

2.1. Molecular cloning, protein expression and purification

Total RNA was isolated from adult *A. lumbricoides* worms. Double-stranded cDNA was obtained by RT-PCR from total RNA using a reverse transcription system (Promega). The gene encoding Al-CPI (GenBank accession No. HQ404231) was amplified by PCR from cDNA with the primers 5′-CCG**GAATTC**GAAAACCTGTA-TTTTCAGGGCCAAGTAGGAGTTCCTGGTGGTTTC-3′ and 5′-ACGC**GTCGAC**TTATGCAGATTTGCATTCTTTGATG-3′ (*Eco*RI and *Sal*I sites, respectively, are shown in bold). The purified PCR

product was digested with *Eco*RI and *Sal*I and ligated into a similarly digested pET28a vector (Novagen). The resulting construct contained an additional tobacco etch virus (TEV) cleavage site (Glu-Asn-Leu-Tyr-Phe-Gln/Gly) between the His tag and the protein-coding sequence. The resulting plasmid was confirmed by DNA sequencing (Invitrogen).

The recombinant plasmid pET28a-Al-CPI was transformed into *Escherichia coli* BL21 (DE3) cells (Novagen). Cells were grown at 310 K in Luria–Bertani (LB) medium containing 100 µg ml^{-1} kanamycin to an OD_{600} of 0.6–0.8. Protein expression was induced with 0.8 m*M* isopropyl *β*-D-1-thiogalactopyranoside (IPTG) for 20 h at 293 K. The cells were harvested by centrifugation at 6000*g* for 10 min at 277 K and frozen at 193 K until purification. The cells were resuspended in 20 m*M* Tris–HCl, 200 m*M* NaCl pH 7.8 and lysed by three passes through a JN-3000 PLUS cell disrupter (JNBIO) at 135 MPa. The lysed cells were then centrifuged at 18 000*g* for 30 min at 277 K. The supernatant was loaded onto a nickel–nitrilotriacetic acid (Ni–NTA) column (Qiagen). The column was washed with ten column volumes of 20 m*M* Tris–HCl, 200 m*M* NaCl and 50 m*M* imidazole pH 7.8 to remove contaminants. Al-CPI was then eluted with 20 m*M* Tris–HCl, 200 m*M* NaCl and 250 m*M* imidazole pH 7.8. The N-terminal His tag was cleaved off with TEV protease overnight at 289 K while dialysing the solution against 20 m*M* Tris–HCl, 50 m*M* NaCl pH 7.8. The cleaved protein mixture was loaded onto an Ni–NTA column (Qiagen). The flowthrough fraction was concentrated to about 5 ml using a Millipore Amicon Ultra-15 centrifugal filter (3000 Da molecular-weight cutoff) and loaded onto a HiLoad 16/60 Superdex 75 gel-filtration column (GE Healthcare) pre-equilibrated with 20 m*M* Tris–HCl, 100 m*M* NaCl and 5% glycerol pH 7.4. The peak fractions containing the target protein were collected and concentrated. The protein concentration was determined using the Bradford assay (Bradford, 1976). The result of each purification step was monitored by SDS–PAGE.

2.2. Crystallization

The target protein was concentrated to 30 mg ml^{-1} by ultrafiltration (Millipore Amicon) in a buffer consisting of 20 m*M* Tris–HCl, 100 m*M* NaCl and 5% glycerol pH 7.4. Crystallization experiments were performed using the sitting-drop vapour-diffusion method at 293 K in 96-well plates (Greiner). Crystal Screen HT, Index HT, SaltRx HT, PEG/Ion HT (Hampton Research), Wizard I, Wizard II and Wizard III (Emerald BioSystems) were used to screen for initial crystallization conditions. 1 µl protein solution was mixed with 1 µl reservoir solution and equilibrated against 70 µl reservoir solution. Crystals appeared several days later in a condition (condition C4 of Crystal Screen HT) consisting of 0.2 *M* sodium acetate, 0.1 *M* sodium cacodylate pH 6.5, 30% PEG 8000. No optimization of the crystallization condition was needed and the diffraction quality of the crystal was sufficient for data collection.

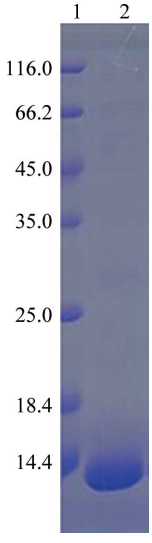

Figure 1
15% SDS–PAGE analysis of Al-CPI. Lane 1, markers (kDa); lane 2, eluted fraction containing Al-CPI from the HiLoad 16/60 Superdex 75 gel-filtration column.

2.3. Data collection

The Al-CPI crystal was sequentially immersed in crystallization solution containing an additional 5, 10, 15 and 20%(*v*/*v*) ethylene glycol as cryoprotectant. The looped crystal was then cooled in a

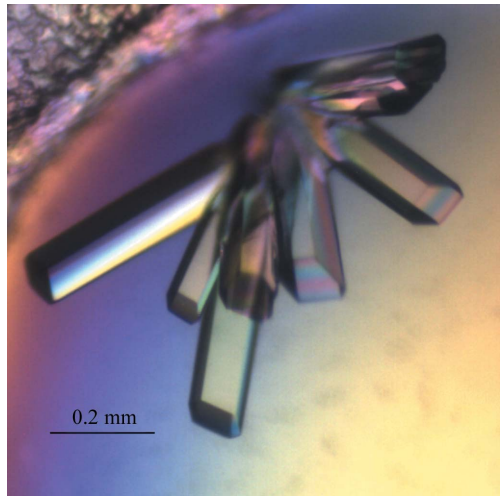

Figure 2
Crystals of Al-CPI obtained using the sitting-drop vapour-diffusion method.

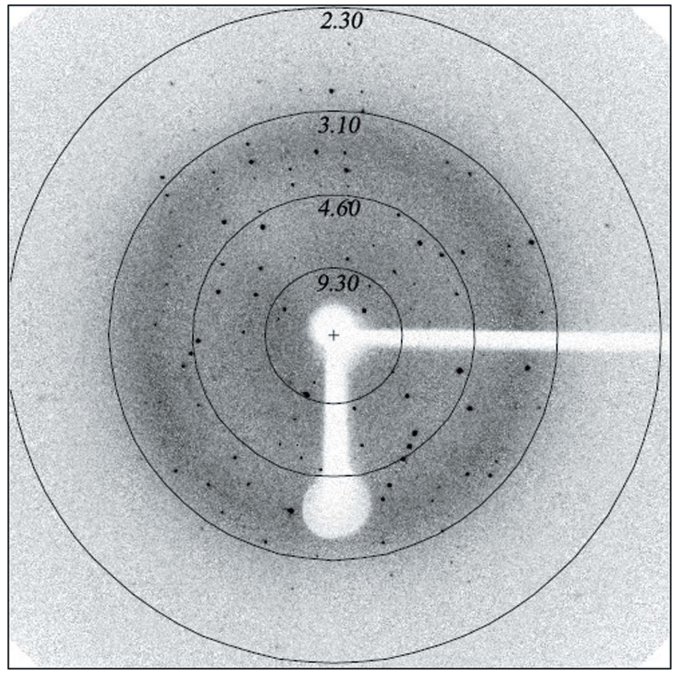

Figure 3
X-ray diffraction image from an Al-CPI crystal with resolution circles marked in Å.

Table 1
Data-collection statistics for the Al-CPI crystal.

Values in parentheses are for the highest resolution shell.

Space group	*C*2
Unit-cell parameters (Å, °)	a = 99.40, b = 37.52, c = 62.92, β = 118.26
Wavelength (Å)	1.54056
Temperature (K)	100
Resolution range (Å)	18.46–2.10 (2.21–2.10)
Unique reflections	12136 (1766)
Multiplicity	5.7 (3.1)
Average $I/\sigma(I)$	10.1 (2.3)
Completeness (%)	99.7 (99.1)
$R_{\rm merge}$ (%)	13.0 (50.3)
Matthews coefficient (Å^3 Da^{-1})	2.03
Solvent content (%)	39.52

liquid-nitrogen stream maintained at 100 K and subjected to X-ray diffraction data collection. A complete diffraction data set consisting of 462 frames was collected at 100 K using an in-house Oxford Diffraction Gemini R Ultra system with a 135 mm Ruby CCD detector at the Guangzhou Institutes of Biomedicine and Health, Chinese Academy of Sciences. Diffraction data were indexed and integrated using *MOSFLM* (Leslie, 1992) and scaled using *SCALA* from the *CCP*4 program suite (Collaborative Computational Project, Number 4, 1994).

3. Results and discussion

Recombinant Al-CPI was expressed in a soluble form in *E. coli* at 293 K. About 10 mg of Al-CPI could be purified from a litre of cell culture and the purity of Al-CPI was more than 95% as determined by SDS–PAGE (Fig. 1). The purified Al-CPI was concentrated to 30 mg ml^{-1} for crystal screening. Several days after high-throughput crystallization screening, diffraction-quality crystals were obtained using the sitting-drop vapour-diffusion method from a condition consisting of 0.2 *M* sodium acetate, 0.1 *M* sodium cacodylate pH 6.5, 30% PEG 8000. An image of typical Al-CPI crystals is shown in Fig. 2. A diffraction data set was collected to 2.10 Å resolution (Fig. 3).

The crystal belonged to the *C*-centred monoclinic space group *C*2, with unit-cell parameters a = 99.40, b = 37.52, c = 62.92 Å, β = 118.26°. Diffraction data for Al-CPI were processed in the resolution range 18.46–2.10 Å. There were predicted to be two Al-CPI molecules in the asymmetric unit, corresponding to a Matthews coefficient of 2.03 Å^3 Da^{-1} and a solvent content of 39.52% (Matthews, 1968). A summary of the crystal parameters and the statistics of the diffraction data are presented in Table 1. An initial molecular-replacement solution was obtained using chicken egg-white cystatin (PDB code 1cew; Bode *et al.*, 1988), which has 34% sequence identity to Al-CPI, as a search model with the program *BALBES* (Long *et al.*, 2008). Further model improvement and refinement is in progress. The crystal structure of Al-CPI should facilitate understanding of the role of Al-CPI in immune response.

This work was supported by grants from the One Hundred Person Project of the Chinese Academy of Sciences, the Knowledge Innovation Program of the Chinese Academy of Sciences (KSCX2-YW-R-084) and the National Natural Science Foundation of China (30872370).

References

Bode, W., Engh, R., Musil, D., Thiele, U., Huber, R., Karshikov, A., Brzin, J., Kos, J. & Turk, V. (1988). *EMBO J.* **7**, 2593–2599.
Bradford, M. M. (1976). *Anal. Biochem.* **72**, 248–254.
Chapman, H. A., Riese, R. J. & Shi, G.-P. (1997). *Annu. Rev. Physiol.* **59**, 63–88.
Collaborative Computational Project, Number 4 (1994). *Acta Cryst.* D**50**, 760–763.
Dainichi, T., Maekawa, Y., Ishii, K., Zhang, T., Nashed, B. F., Sakai, T., Takashima, M. & Himeno, K. (2001). *Infect. Immun.* **69**, 7380–7386.
Gregory, W. F. & Maizels, R. M. (2008). *Int. J. Biochem. Cell Biol.* **40**, 1389–1398.
Honey, K. & Rudensky, A. Y. (2003). *Nature Rev. Immunol.* **3**, 472–482.
Leslie, A. G. W. (1992). *Jnt CCP4/ESF–EACBM Newsl. Protein Crystallogr.* **26**.
Long, F., Vagin, A. A., Young, P. & Murshudov, G. N. (2008). *Acta Cryst.* D**64**, 125–132.
Lustigman, S., Brotman, B., Huima, T., Prince, A. M. & McKerrow, J. H. (1992). *J. Biol. Chem.* **267**, 17339–17346.
Matthews, B. W. (1968). *J. Mol. Biol.* **33**, 491–497.
Schonemeyer, A., Lucius, R., Sonnenburg, B., Brattig, N., Sabat, R., Schilling, K., Bradley, J. & Hartmann, S. (2001). *J. Immunol.* **167**, 3207–3215.
Turk, B., Stoka, V., Rozman-Pungerčar, J., Cirman, T., Droga-Mazovec, G., Orešić, K. & Turk, V. (2002). *Biol. Chem.* **383**, 1035–1044.
Turk, B., Turk, V. & Turk, D. (1997). *Biol. Chem.* **378**, 141–150.